Quantitative Evaluations of Posterior Staphylomas in Highly Myopic Eyes by Ultra-Widefield Optical Coherence Tomography

Noriko Nakao, Tae Igarashi-Yokoi, Hiroyuki Takahashi, Shiqi Xie, Kosei Shinohara, and Kyoko Ohno-Matsui

Department of Ophthalmology and Visual Science, Tokyo Medical and Dental University, Tokyo, Japan

Correspondence: Tae Igarashi-Yokoi, Department of Ophthalmology and Visual Science, Tokyo Medical and Dental University, 1-5-45 Yushima, Bunkyo-ku, Tokyo 113-8510, Japan; yokoitae@icloud.com.

Received: August 8, 2021
Accepted: June 30, 2022
Published: July 22, 2022

Citation: Nakao N, Igarashi-Yokoi T, Takahashi H, Xie S, Shinohara K, Ohno-Matsui K. Quantitative evaluations of posterior staphylomas in highly myopic eyes by ultra-widefield optical coherence tomography. *Invest Ophthalmol Vis Sci.* 2022;63(8):20. https://doi.org/10.1167/iovs.63.8.20

Purpose. To determine the shape of posterior staphylomas using ultra-widefield optical coherence tomographic (UWF-OCT) images and to identify the factors contributing to the shape and grade of the staphylomas in eyes with pathologic myopia.

Methods. This was an observational case series study. Highly myopic patients who were ≥40 years old with wide or narrow type of macular staphylomas were studied. High myopia was defined as a myopic refractive error (spherical equivalent) greater than −8.0 diopters (D) or an axial length (AL) > 26.5 mm. The maximum diameter and depth of the staphylomas were measured in the 12 radial scans of UWF-OCT images by ImageJ software and were compared between the two types of staphylomas.

Results. We studied 197 eyes of 138 patients with a mean age of 64.7 ± 10.4 years and mean AL of 30.0 ± 1.9 mm. The AL was significantly longer in the eyes with the narrow type than the wide type of staphyloma ($P = 0.036$). Multiple regression analyses showed that age was significantly correlated with the maximum depth/maximum diameter ratio (wide type, $P < 0.001$; narrow type, $P = 0.003$) of both types of staphylomas. The AL was significantly correlated with the depth/diameter ratio of only the narrow type of staphylomas ($P = 0.005$).

Conclusions. The significant correlations of age and AL with the wide and narrow types of posterior staphylomas indicate that the factors for their formations may be distinctly different. Quantitative analyses of UWF-OCT images are helpful in determining the shape of the staphylomas.

Keywords: posterior staphylomas, pathologic myopia, ultra-widefield optical coherence tomography

A posterior staphyloma is an outpouching of a circumscribed region of the posterior pole of the eye, and its presence has been considered to be a hallmark of pathologic myopia.[1–4] Posterior staphylomas have been confused with generalized scleral bowing due to an axial elongation; however, Spaide[5] resolved this difficulty by presenting a clear definition of a staphyloma; he defined a staphyloma as an outpouching of a region of the posterior fundus with a radius of curvature that was shorter than the radius of curvature of the adjacent eye wall.

Several methods have been used to detect and classify the types and grades of staphylomas. Earlier, color fundus photographs, ultrasonographic images, or a combination of both were used to detect and classify staphylomas.[3] However, most staphylomas involve wide areas of the fundus; thus, the entire extent of staphylomas did not fit within the 50° field of view of conventional fundus photographs.

To overcome these difficulties, our research laboratory has used three-dimensional magnetic resonance imaging of the eye in which the entire extent of staphylomas could be imaged, resulting in a more accurate view of the shape of the whole eye.[3,6,7] However, this was not feasible as a screening technique due to its relatively low spatial resolution, which makes subtle changes of shallow staphylomas difficult to detect.

Although optical coherence tomography (OCT) is a helpful method to analyze the curvature of the sclera in eyes with pathologic myopia,[8,9] the limited scanned area made it not possible to view the entire extent of the staphylomas. To overcome this limitation, Shinohara et al.[10] used an ultra-widefield OCT (UWF-OCT) prototype with 23-mm wide and 5-mm deep scans. They succeeded in imaging the entire extent of staphylomas. They found that the staphyloma edges had three consistent OCT features: a gradual choroidal thinning toward the staphyloma edge, an inward protrusion of the sclera, and a posterior displacement of sclera in the area posterior to the edges. Based on these features, more accurate determinations of the presence and the extent of staphylomas have been possible.

Quantitative evaluations of the shape and the depth of staphylomas are important parameters to analyze to

determine the progression of staphylomas and to analyze their risks of damaging the retina and optic nerve. In addition, quantitative evaluations of staphylomas are important for the analyses of the sclera-targeted therapies against posterior staphylomas, such as scleral reinforcement, scleral collagen crosslinking, and scleral regeneration therapy.[11–13] However, a search of PubMed extracted only a few quantitative studies of the shape of posterior staphylomas and the factors associated with the shapes. Frisina et al.[14] measured the width and the depth of posterior staphylomas using the vertical and the horizontal B-scan ultrasound images in 90 eyes of 67 patients with high myopia and a posterior staphyloma. They reported that there was a significant correlation between the depth and diameter of posterior staphylomas. However, B-scan ultrasound examinations of the entire area of a large staphyloma are difficult, and they cannot detect the staphyloma edges accurately unless the staphyloma becomes very prominent.

The UWF-OCT devices can obtain images that show the more subtle changes of the scleral curvature better than B-mode echography images. Their higher resolution has allowed clinicians to identify the staphyloma edges based on the three OCT features as reported by Shinohara et al.[11] In addition, 12 radial scans of the UWF-OCT centered on the fovea can be thoroughly examined to determine the maximum depth and the maximum diameter of the staphylomas.

Thus, the purpose of this study was to identify the staphyloma edges and the most protruded point of staphylomas based on the 12 radial scans of UWF-OCT and to measure the parameters regulating the shape of staphylomas. Factors contributing to the shape and the grade of the staphylomas, as well as the correlation with the myopic maculopathy lesions, were also investigated.

Materials and Methods

Subjects

The procedures used in this study conformed to the tenets of the Declaration of Helsinki and were approved by the Ethics Committee of Tokyo Medical and Dental University (approval no. M2000-2278). A signed informed consent was obtained from all subjects.

Highly myopic patients who were ≥40 years old with wide or narrow types of macular posterior staphylomas were studied. All had been examined by UWF-OCT between February and July 2017. High myopia was defined as a myopic refractive error (spherical equivalent) greater than −8.0 diopters (D), or an axial length (AL) longer than 26.5 mm, according to the definition of the Ministry of Health and Welfare, Japan. The exclusion criteria were poor-quality OCT images, prior vitreoretinal surgery, presence of a dome-shaped macula (DSM), and an inward bulging of the retinal pigment epithelium (RPE) with a maximal height >50 µm above a line connecting the RPE borders in the UWF-OCT images.[15–17]

All patients had undergone comprehensive ophthalmological examinations including measurements of the best-corrected visual acuity (BCVA), refractive error, and AL (IOLMaster; Carl Zeiss Meditec, Jena, Germany). Dilated stereoscopic fundus examinations and color fundus photography using the TRC-50DX retinal camera (Topcon, Tokyo, Japan) or Optos 200Tx scanning laser ophthalmoscope (Optos, Dunfermline, UK) were performed on all eyes.

Ultra-Widefield OCT

UWF-OCT images were obtained with a prototype swept-source UWF-OCT instrument (Canon, Tokyo, Japan) with an A-scan repetition rate of 100,000 Hz. The light source was a tunable laser centered at 1050 nm with a 100-nm tuning range. The length of the scanned line was 78° horizontally and 68° vertically. The field of view was 23 mm × 20 mm, and the scan depth was 5.3 mm. Cross-sectional scans and 12 radial scans centered on the fovea were obtained.

The staphyloma types were classified based on UWF-OCT images according to those reported by Ohno-Matsui et al.[3] and by Shinohara et al.[10] (Supplementary Fig. S1). The detection of a staphyloma was made by identifying the staphyloma edges. As reported by Shinohara et al.,[10,18] staphyloma edges had three consistent features; a gradual thinning of the choroid from the periphery toward the edge of the staphyloma, a gradual rethickening of the choroid in a direction toward the posterior pole, and an inward protrusion of the sclera at the staphyloma edges in the UWF-OCT images. In addition, the posterior displacement of the staphylomatous area compared to the surrounding area was considered an important characteristic that was used for the diagnosis and classification of the staphylomas. Earlier studies reported that two types of staphylomas were dominant: a wide macular type that was equivalent to Curtin's type I and a narrow macular type that was equivalent to Curtin's type II.[1,3,14] Thus, the measurements were performed on eyes with these two types of staphylomas.

Measurements of Maximum Diameter and Depth of Staphylomas

The maximum diameter and maximum depth of a posterior staphyloma in the UWF-OCT images were measured with ImageJ (National Institutes of Health, Bethesda, MD, USA). We equalized the aspect ratio of pixel resolution and corrected the magnification by ImageJ before the measurements. We measured the distance in pixels and converted it to micrometers by multiplying the distance by the factor of the horizontal pixel resolution (Supplementary Fig. S2). The maximum diameter was defined as the longest line connecting the edges of the posterior staphylomas in one of the 12 radial scans (Fig. 1). The maximum depth was defined as the longest line perpendicular to the maximum diameter in the same scan. The lengths were measured in pixel units. The horizontal and vertical OCT sections that crossed the fovea were used for the measurements of the choroidal thickness. The measurements of the subfoveal choroidal thickness were performed by one masked examiner (NN).

Statistical Analyses

SPSS Statistics 22.0 (IBM, Inc., Chicago, IL, USA) was used for all statistical analyses. We analyzed the BCVA, refractive error, AL, maximum diameter, maximum depth, ratio of the maximum depth to the maximum diameter (depth/diameter) of the posterior staphylomas, and the subfoveal choroidal thickness. These values were compared between the eyes with the wide type and those with the narrow type of macular staphylomas. Student's *t*-tests, Welch's *t*-tests, and Mann–Whitney *U* tests were used to determine the significance of the differences. We also determined the significance of

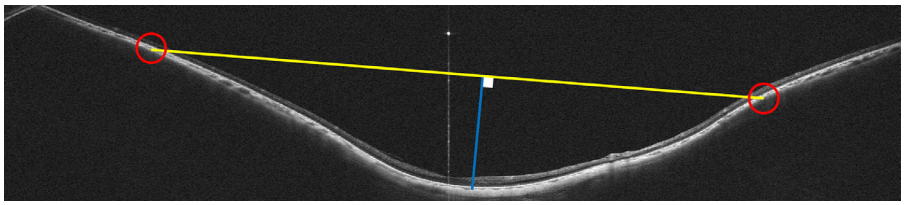

Figure 1. Example of how the maximum diameter and maximum depth were measured by ImageJ. This UWF-OCT image is one of the 12 radial scans of the eye. The *red circle* indicates the edge of the posterior staphyloma. The posterior staphyloma edge was identified based on the characteristics of the posterior staphyloma edge described in the paper by Shinohara et al.[10] as an area with a gradual thinning of the choroid from the periphery toward the edge of the staphyloma, a gradual rethickening of the choroid in a direction toward the posterior pole, and an inward protrusion of the sclera. ImageJ was used to measure the line segments connecting the edges indicated by the *yellow lines*. Of the 12 images of the radial scans, the longest line segment was selected as the maximum diameter. The maximum depth was defined as the longest line segment perpendicular to the maximum diameter, as indicated by the *blue line*.

the differences in the myopic macular neovascularization (MNV), myopic traction maculopathy (MTM), myopic optic neuropathy (MON), glaucomatous optic neuropathy (GON), ratio of MON to GON, lacquer cracks, patchy atrophy, and macula atrophy by χ^2 tests in the wide type and narrow type of staphylomas. The diagnosis of MTM was made by the presence of epiretinal traction and changes in the retinal structure according to the criteria reported by Panozzo et al.[19] MON and GON were diagnosed by the presence of visual field defects due to a stretching and distortion of the optic disc in highly myopic or glaucomatous eyes when the impact of the retinal lesions on the visual fields was not detected.[20] MNV, lacquer cracks, patchy atrophy, and macula atrophy were diagnosed according to the META-PM classification.[21]

The characteristics of the two types of staphylomas were analyzed separately. For each type of staphyloma, we compared the characteristics of the diameter/depth ratio of the staphyloma at different ages (40–64 years vs. >65 years) and for different ALs (≤30.0 mm vs. >30.0 mm). The correlations of the diameter/depth ratio of the staphyloma and age or AL were determined by Pearson's tests and Spearman's rank tests.

Multiple regression analyses were used to determine the significance of the correlations between the diameter/depth ratio of the staphyloma and the various ocular characteristics. The dependent variables were the diameter/depth ratio of the staphyloma, and the independent variables were age, AL, BCVA expressed in logarithm of minimal angle of resolution (logMAR) units, and subfoveal choroidal thickness. In addition, the myopic MNV, MTM, MON/GON, lacquer cracks, patchy atrophy, and macula atrophy were analyzed. $P < 0.05$ was considered statistically significant.

Results

The medical records of 244 eyes of 173 consecutive patients with high myopia were analyzed. Forty-two eyes of 31 patients with DSM, two eyes of two patients with prior vitreoretinal surgery, and three eyes of two patients with poor-quality UWF-OCT images were excluded. Of the remaining 138 patients (197 eyes), 39 patients (59 eyes) were men and 99 (138 eyes) were women. Of the 197 eyes, 102 eyes (51.8%) had the wide type of macula staphyloma and 95 of the 197 eyes (48.2%) had the narrow type of macular staphyloma ($P > 0.05$). The mean age of all patients was 64.7 ± 10.4

Table 1. Comparisons of Clinical Characteristics of Eyes With Wide and Narrow Types of Macular Posterior Staphyloma

	Macular Type		
	Wide	**Narrow**	***P***
Eyes (patients), *n*	102 (80)	95 (73)	—
Age (y), mean ± SD (range)	63.3 ± 10.1 (42–80)	65.2 ± 11.0 (42–89)	0.215
BCVA (logMAR), mean ± SD (range)	0.30 ± 0.48 (−0.18 to 2.0)	0.26 ± 0.47 (−0.18 to 2.0)	0.428
Refractive error (D), mean ± SD (range)	−13.0 ± 3.6 (−21.9 to −5.8)	−12.5 ± 6.0 (−27.0 to −6.5)	0.802
AL (mm), mean ± SD (range)	29.7 ± 1.7 (25.2–33.2)	30.3 ± 2.1 (26.8–35.9)	0.036*
Subfoveal choroid (μm), mean ± SD (range)	43.3 ± 27.2 (0–119)	42.1 ± 23.1 (0–191)	0.311
Maximum diameter (μm), mean ± SD (range)	20193 ± 2208 (14,864–24,847)	14749 ± 2569 (8288–20,536)	<0.001*
Maximum depth (μm), mean ± SD (range)	3214 ± 574 (1786 to 4254)	2608 ± 704 (1121–4226)	<0.001*
Maximum depth/maximum diameter ratio, mean ± SD (range)	0.16 ± 0.02 (0.10–0.23)	0.18 ± 0.03 (0.11–0.28)	<0.001†
MNV (eyes)	24 (23.5%)	22 (23.2%)	0.951
MTM (eyes)	37 (36.3%)	37 (38.9%)	0.699
MON/GON ratio (eyes)	30 (29.4%)	48 (50.5%)	0.002‡
Lacquer crack (eyes)	17 (16.7%)	23 (24.2%)	0.188
Patchy atrophy (eyes)	25 (24.5%)	30 (31.6%)	0.269
Macula atrophy (eyes)	17 (16.7%)	13 (13.7%)	0.560

* Student's *t*-test.
† Welch's *t*-test.
‡ χ^2 test.

Investigative Ophthalmology & Visual Science

Table 2. Comparisons of Three Parameters of Posterior Staphylomas as a Function of Age and AL in Wide and Narrow Types of Macular Posterior Staphylomas

	Age (y)			AL (mm)		
	40–64	≥65	*P*	26.6–30	>30	*P*
Wide Macular Staphyloma Type						
Eyes (patients), *n*	50 (35)	52 (45)	–	59 (48)	43 (38)	–
Maximum depth/maximum diameter ratio, mean ± SD (range)	0.15 ± 0.02 (0.11–0.21)	0.17 ± 0.02 (0.10–0.23)	<0.001	0.16 ± 0.03 (0.10–0.23)	0.16 ± 0.02 (0.12–0.20)	0.658
Narrow Macular Staphyloma Type						
Eyes (patients), *n*	38 (29)	57 (44)	–	44 (33)	51 (42)	–
Maximum depth/maximum diameter ratio, mean ± SD (range)	0.17 ± 0.03 (0.11–0.23)	0.18 ± 0.03 (0.12–0.28)	0.040*	0.17 ± 0.04 (0.11–0.28)	0.18 ± 0.03 (0.13–0.24)	0.046*

* Student's *t*-test.

years with a range of 42 to 89 years. The mean refractive error (spherical equivalent) was −10.8 ± 2.9 diopters (D) with a range of −13.0 to −4.0 D. The mean AL was 30.0 ± 1.9 mm with a range of 25.2 to 35.9 mm.

The characteristics of eyes with the wide type and the narrow type of macular staphylomas are shown in Table 1. There were no significant differences in age, BCVA, or refractive error between the two groups. The AL was significantly longer in the eyes with the narrow type than in eyes with the wide type of macular staphylomas (30.3 ± 2.1 mm vs. 29.7 ± 1.7 mm; $P = 0.036$). The MON/GON ratio was significantly greater in the eyes with the narrow type than in the eyes with the wide type of macular staphylomas (48/95 vs. 30/102; $P = 0.002$). The differences in the incidences of MNV, MTM, patchy atrophy, lacquer cracks, and other myopic complications were not significant. The difference in the subfoveal choroidal thickness between the two groups was also not significant. The maximum diameter, maximum depth, and depth/diameter ratio were significantly greater in eyes with the narrow type of macular staphyloma than eyes with the wide type of macular staphyloma (14,749 ± 2569 µm vs. 20,193 ± 2208 µm, $P < 0.001$; 2608 ± 704 µm vs. 3214 ± 574 µm, $P < 0.001$; 0.18 ± 0.03 vs. 0.16 ± 0.02, $P < 0.001$, respectively). We compared the characteristics of the three parameters of the posterior staphylomas as a function of age (40–64 years vs. >65 years) and AL (≤30.0 mm vs. >30.0 mm) as shown in Table 2.

Influence of Age on Parameters Associated With Shape of Staphylomas

In the wide type of macular staphyloma, the patients older than 65 years had a significantly higher depth/diameter ratio than those who were 40 to 64 years old (0.17 ± 0.02 vs. 0.15 ± 0.02; $P < 0.001$) (Figs. 2, 3). In the patients with narrow macular staphylomas, the patients older than 65 years had slightly but significantly higher depth/diameter ratios than those who were 40 to 64 years old (0.18 ± 0.03 vs. 0.17 ± 0.03; $P = 0.040$).

Effect of AL on Parameters Regulating Shape of Staphylomas

In the eyes with the wide type of macular staphyloma, there was no significant difference in the depth/diameter ratio between the two AL groups. In the eyes with the narrow

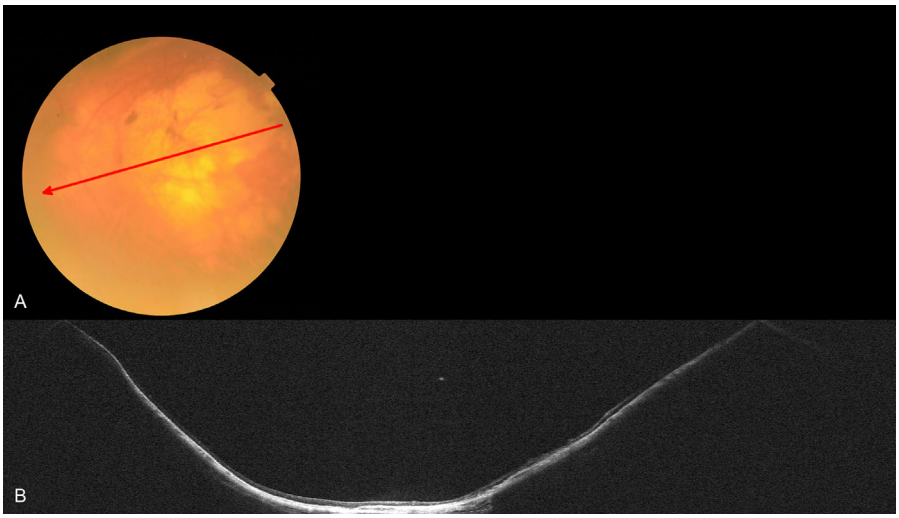

Figure 2. UWF-OCT images of highly myopic eyes of patients >65 years with the wide type of macular staphyloma. (**A**) Fundus photograph of the left eye of an 89-year-old woman with an AL of 29.2 mm. The *red arrow* points to an UWF-OCT image. (**B**) UWF-OCT image of a wide type of macular posterior staphyloma. The maximum depth/maximum diameter ratio of the posterior staphyloma is 0.22.

Investigative Ophthalmology & Visual Science

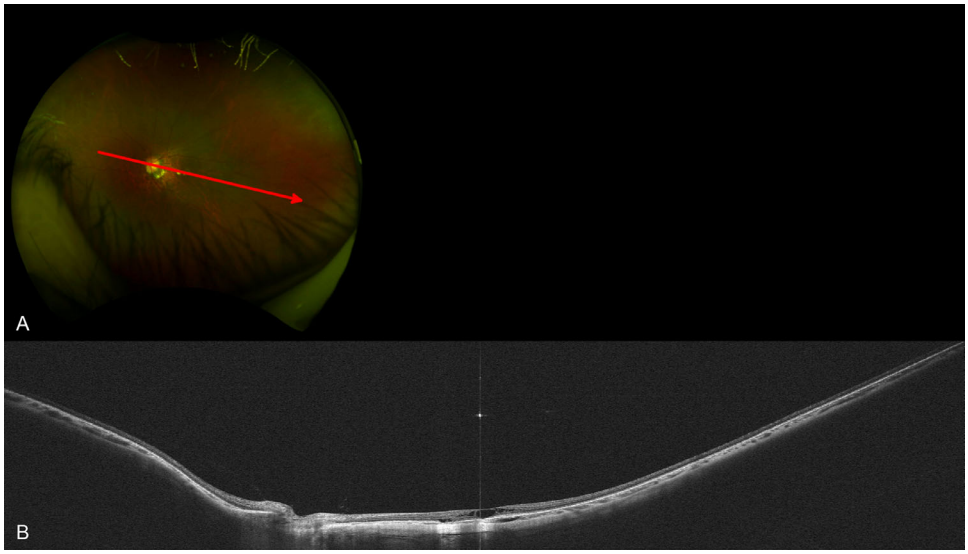

Figure 3. UWF-OCT images of a highly myopic eye of 40- to 64-year-old patients with the wide type of macular staphyloma. (**A**) Fundus photograph of the left eye of a 46-year-old woman with an AL of 28.4 mm. The *red arrow* points to the direction of the scan for the UWF-OCT image. (**B**) UWF-OCT image showing a wide type of macular posterior staphyloma. The maximum depth/maximum ratio of the posterior staphyloma is 0.12.

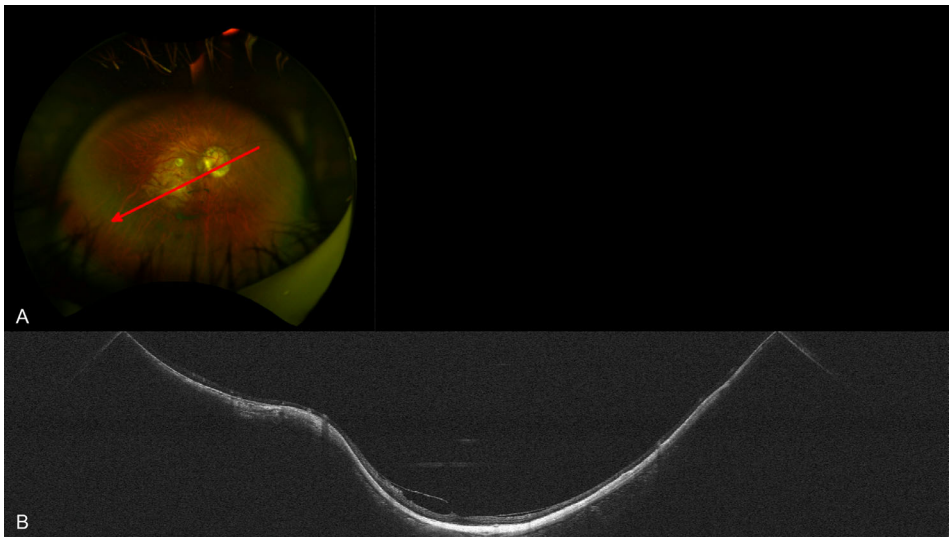

Figure 4. UWF-OCT images of a highly myopic eye of a patient with the narrow type of macular staphyloma. The AL was >30.0 mm. (**A**) Fundus photograph of the right eye of a 60-year-old man with an AL of 35.9 mm. The *red arrow* points in the direction of scan for the UWF-OCT image. (**B**) UWF-OCT image of a wide type of macular posterior staphyloma. The maximum depth/maximum diameter ratio of the posterior staphyloma is 0.23.

type of macular staphylomas, the eyes with ALs > 30.0 mm had significantly higher depth/diameter ratios than the eyes with ALs ≤ 30.0 mm (0.18 ± 0.03 vs. 0.17 ± 0.04; $P = 0.046$) (Figs. 4, 5).

Scatterplots and correlations between the diameter/depth ratio of the posterior staphylomas and age and AL are shown in Figure 6. In the eyes with the wide type of macular staphylomas (Figs. 6A–6D), there was a significant correlation between the depth/diameter ratio and age ($r = 0.463$; $P < 0.001$, Pearson's test). The correlation of the depth/diameter ratio of the staphylomas and AL was not significant.

In the eyes with the narrow type of macular staphyloma, a significant correlation was found between the diameter/depth ratio of the posterior staphylomas and age ($r = 0.226$; $P = 0.028$, Pearson's test). The depth/diameter ratio was also positively and significantly correlated with the AL ($r = 0.255$; $P = 0.013$, Spearman's rank tests).

The results of multiple regression analysis showed that, in the wide type of macular staphyloma, only age had significant correlation with the diameter/depth ratio ($R^2 = 0.215$; $P < 0.001$). In contrast, the AL was correlated significantly with the diameter/depth ratio in the narrow type of macular staphyloma ($R^2 = 0.080$; $P = 0.005$). Age and MNV were also correlated significantly with the ratio ($R^2 = 0.145$, $P = 0.003$; $R^2 = 0.192$, $P = 0.025$, respectively) (Table 3) in the narrow type of macular staphyloma.

Investigative Ophthalmology & Visual Science

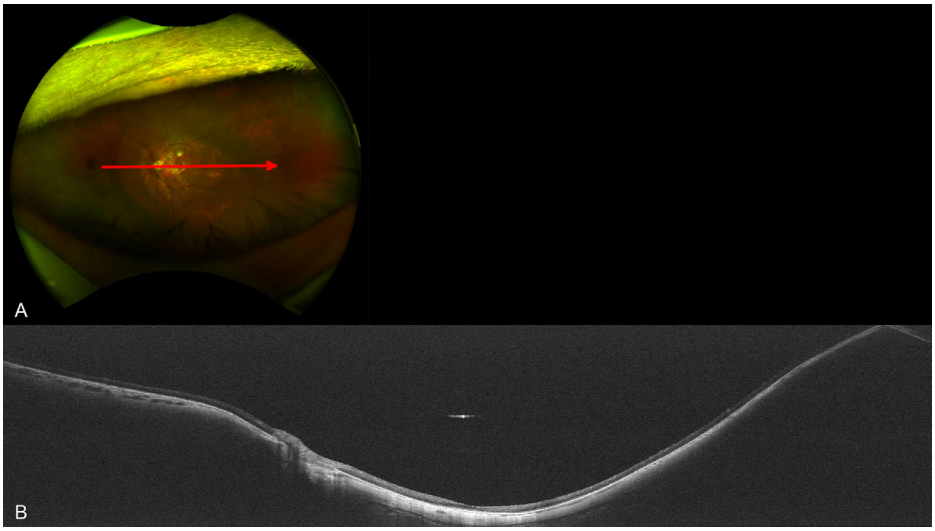

Figure 5. UWF-OCT images of a highly myopic eye with an AL ≤ 30.0 mm of a patient with the narrow type of macular staphyloma. (**A**) Fundus photograph of the left eye of a 70-year-old woman with an AL of 26.8 mm. The *red arrow* shows the direction of the scan for the UWF-OCT image. (**B**) UWF-OCT image showing a wide type of macular posterior staphyloma. The maximum depth/maximum diameter ratio of the posterior staphyloma is 0.17.

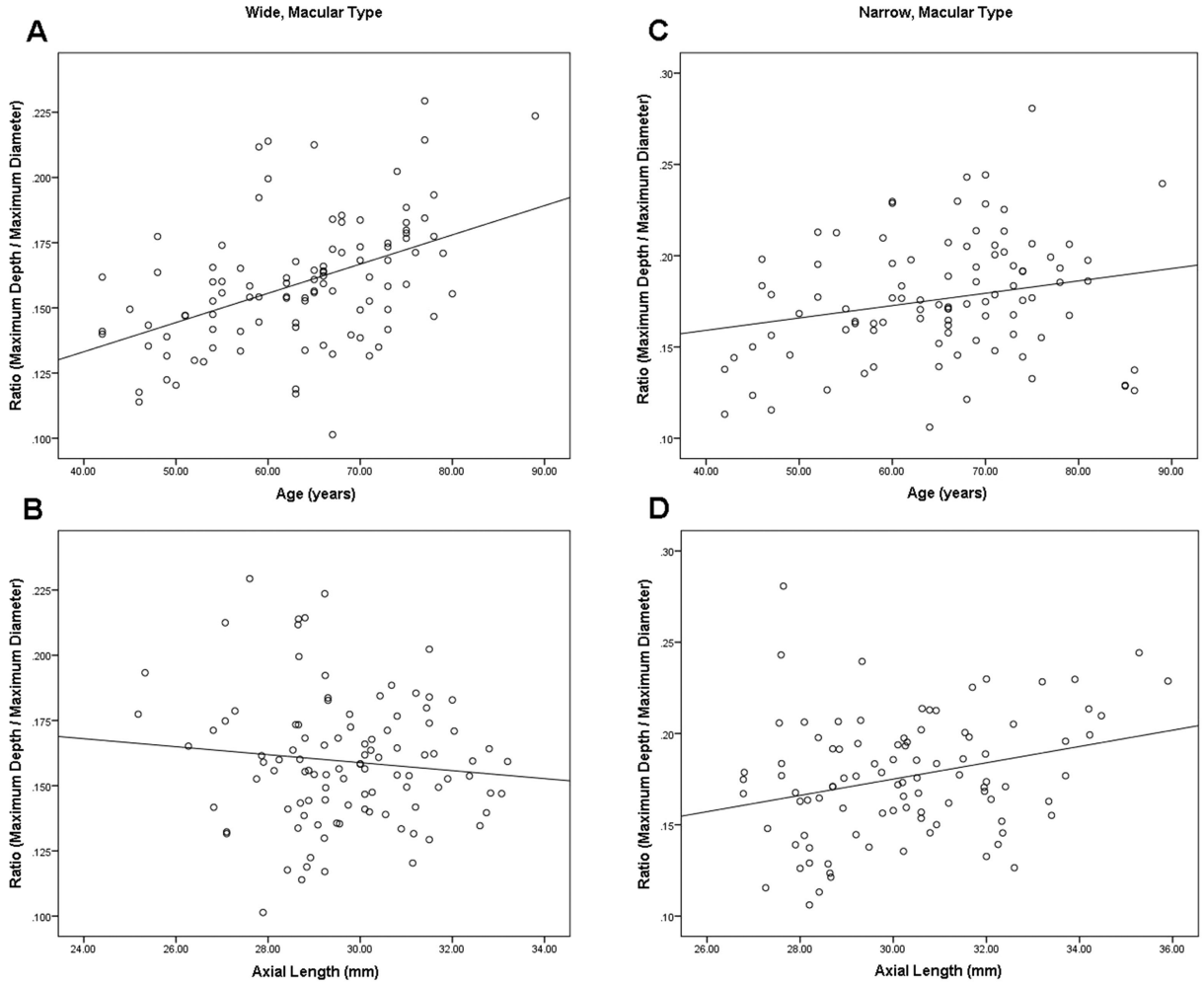

Figure 6. Scatterplots showing the relationships between the maximum depth/maximum diameter ratio and age and AL. (**A**) There is a significant and positive correlation between the maximum depth/maximum diameter ratio and age (years) for the wide type of macular staphyloma ($y = 0.09 + 0.001x$). (**B**) There is no significant correlation between the maximum depth/maximum diameter ratio and the AL (mm) for the wide type of macular staphyloma. (**C**) There is a significant and positive correlation between the maximum depth/maximum diameter ratio and age (years) for the narrow and wide types of macular staphylomas ($y = 0.13 + 0.0007x$). (**D**) There is a significant and positive correlation between the maximum depth/maximum diameter ratio and AL (mm) for the narrow type of macular staphyloma ($y = 0.04 + 0.004x$).

Investigative Ophthalmology & Visual Science

Table 3. Multiple Regression Analysis of Factors in Eyes With Wide and Narrow Types of Macular Staphyloma

Macular Type	Dependent Variable	Independent Variable	R^2	*B*	*P*
Wide	Ratio (maximum diameter/maximum depth)	Age	0.215	0.463	<0.001
Narrow	Ratio (maximum diameter/maximum depth)	AL	0.080	0.279	0.005
		Age	0.145	0.300	0.003
		MNV	0.192	–0.222	0.025

R^2, coefficient of determination; *B*, standardized partial regression coefficient.

Discussion

We obtained images of the entire extent of posterior staphylomas by UWF-OCT and measured the diameter and depth of staphylomas in these images. The depth/diameter ratio was significantly greater in the narrow type than in the wide type of staphylomas. This suggests that the narrow type of macular staphylomas were not simply smaller versions of the wide type of macular staphylomas, but rather the shapes of these two types of staphylomas were distinctly different. The wide type of macular staphyloma tended to have a more gradual protrusion, whereas the narrow type of macular staphylomas tended to have a more abrupt and greater deformity of the posterior sclera (Supplementary Fig. S3).

Interestingly, the patients who were older than 65 years had significantly greater depth/diameter ratios than those who were between 40 and 65 years of age in either type of staphylomas. Multiple regression analyses also showed that age was the main factor significantly associated with the depth/diameter ratio in patients with either type of staphylomas. Although this study was a cross-sectional study and we did not monitor the progression directly, these findings suggest that the wide and narrow types of macular staphyloma deepen with increasing age, although the diameter of the staphylomas remained almost unchanged.

Additionally, multiple regression analyses showed that AL was not correlated with the depth/diameter ratio of the wide macular staphylomas. However, in eyes with the narrow type of macular staphylomas, multiple regression analyses showed that AL was the second most influential factor associated with the depth/diameter ratio, and the depth/diameter ratio was positively correlated with AL. Thus, the longer the eye, the more abrupt were the edges of the narrow staphylomas. Although this study was not a longitudinal study, the results suggest that factors correlated with the progression of staphylomas may be distinctly different between the wide type and narrow type of macular staphylomas.

It is generally believed that highly myopic eyes with staphylomas with more abrupt changes tended to have longer ALs, although it is known that the AL elongation is caused mainly by an expansion of the equatorial region of the eye.[5,22] One hypothesis that could explain our results is that the protrusion of the posterior staphyloma was more likely to occur with an elongation of the AL in eyes with the narrow type of macular staphylomas,. On the other hand, in the wide type of macular staphylomas, the ocular axial elongation was mainly due to an expansion of the equatorial region, and the extension of the eye axis might not directly affect the protrusion of the posterior staphyloma. Thus, an expansion of the equatorial region and the deformity of the posterior sclera are different and independent phenomena with different regions of the eye affected.

Interestingly, our results also showed that, in eyes with the narrow type of macular staphylomas, the depth/diameter ratio of the staphylomas tended to be lower if myopic MNV was present. On the other hand, the existence of myopic MNV was not significantly correlated with the depth/diameter ratio of the staphylomas in eyes with the wide type of macular staphylomas. Several studies have reported that MNV is more frequent in eyes with shallower posterior staphyloma, and the deeper staphylomas had fewer myopic MNVs.[23–25] Although more detailed investigations are required for different posterior staphyloma shapes, our findings suggest that the narrow type of posterior staphylomas may be more prone to develop myopic MNV at a stage where the protrusion of posterior staphyloma is less prominent.

There are some limitations in this study. First, this was not a longitudinal study. Thus, it was not clear whether the pathogenesis and progression of staphylomas were distinctly different between the wide type and the narrow type of macula staphylomas. Second, the measurements of the maximum depth and maximum diameter were based on 12 radial scans. Although the use of 12 radial scans is better than using only vertical and horizontal scans, it is still possible that the most protruded point was located between the radial scans.

In conclusion, the results indicate that successful measurements of the entire depth and width of the staphylomas can be obtained from UWF-OCT images. The parameters significantly associated with the shape of posterior staphylomas can be obtained from these images. The results also showed that the shape of staphylomas and contributing factors for their formations may be distinctly different between the wide type and narrow type of posterior macular staphylomas. Quantitative analyses of the shape of posterior staphylomas were helpful in determining the grade and progression of staphylomas in an objective way. These findings should allow clinicians to predict the anatomical and visual prognosis of patients with pathologic myopia.

Acknowledgments

The authors thank Duco Hamasaki for his critical discussion and final manuscript revision. Supported by grants from the Japanese Society for Promotion of Science (15H04993, 15K15629).

Disclosure: **N. Nakao**, (N); **T. Igarashi-Yokoi**, (N); **H. Takahashi**, (N); **S. Xie**, (N); **K. Shinohara**, (N); **K. Ohno-Matsui,** Santen (F), CooperVision (F)

References

1. Curtin BJ. The posterior staphyloma of pathologic myopia. *Trans Am Ophthalmol Soc*. 1977;75:67–86.

Investigative Ophthalmology & Visual Science

2. Ohno-Matsui K, Jonas JB. Posterior staphyloma in pathologic myopia. *Prog Retin Eye Res*. 2019;70:99–109.
3. Ohno-Matsui K. Proposed classification of posterior staphylomas based on analyses of eye shape by three-dimensional magnetic resonance imaging and wide-field fundus imaging. *Ophthalmology*. 2014;121(9):1798–1809.
4. Flitcroft DI, He M, Jonas JB, et al. IMI - defining and classifying myopia: a proposed set of standards for clinical and epidemiologic studies. *Invest Ophthalmol Vis Sci*. 2019;60(3):M20–M30.
5. Spaide RF. Staphyloma: part 1. In: Spaide RF, Ohno-Matsui K, Yannuzzi LA, eds., *Pathologic Myopia*. New York: Springer; 2014;167–176.
6. Moriyama M, Ohno-Matsui K, Hayashi K, et al. Topographic analyses of shape of eyes with pathologic myopia by high-resolution three-dimensional magnetic resonance imaging. *Ophthalmology*. 2011;118(8):1626–1637.
7. Moriyama M, Ohno-Matsui K, Modegi T, et al. Quantitative analyses of high-resolution 3D MR images of highly myopic eyes to determine their shapes. *Invest Ophthalmol Vis Sci*. 2012;53(8):4510–4518.
8. Ohno-Matsui K, Akiba M, Modegi T, et al. Association between shape of sclera and myopic retinochoroidal lesions in patients with pathologic myopia. *Invest Ophthalmol Vis Sci*. 2012;53(10):6046–6061.
9. Imamura Y, Iida T, Maruko I, Zweifel SA, Spaide RF. Enhanced depth imaging optical coherence tomography of the sclera in dome-shaped macula. *Am J Ophthalmol*. 2011;151(2):297–302.
10. Shinohara K, Shimada N, Moriyama M, et al. Posterior staphylomas in pathologic myopia imaged by widefield optical coherence tomography. *Invest Ophthalmol Vis Sci*. 2017;58(9):3750–3758.
11. Li XJ, Yang XP, Li QM, et al. Posterior scleral reinforcement for the treatment of pathological myopia. *Int J Ophthalmol*. 2016;9(4):580–584.
12. Wollensak G, Iomdina E, Dittert DD, Salamatina O, Stoltenburg G. Cross-linking of scleral collagen in the rabbit using riboflavin and UVA. *Acta Ophthalmol Scand*. 2005;83(4):477–482.
13. Shinohara K, Yoshida T, Liu H, et al. Establishment of novel therapy to reduce progression of myopia in rats with experimental myopia by fibroblast transplantation on sclera. *J Tissue Eng Regen Med*. 2018;12(1):e451–e461.
14. Frisina R, Baldi A, Cesana BM, Semeraro F, Parolini B. Morphological and clinical characteristics of myopic posterior staphyloma in Caucasians. *Graefes Arch Clin Exp Ophthalmol*. 2016;254(11):2119–2129.
15. Ellabban AA, Tsujikawa A, Matsumoto A, et al. Three-dimensional tomographic features of dome-shaped macula by swept-source optical coherence tomography. *Am J Ophthalmol*. 2013;155(2):320–328.
16. Fang Y, Jonas JB, Yokoi T, Cao K, Shinohara K, Ohno-Matsui K. Macular Bruch's membrane defect and dome-shaped macula in high myopia. *PLoS One*. 2017;12(6):e0178998.
17. Caillaux V, Gaucher D, Gualino V, Massin P, Tadayoni R, Gaudric A. Morphologic characterization of dome-shaped macula in myopic eyes with serous macular detachment. *Am J Ophthalmol*. 2013;156(5):958–967.
18. Shinohara K, Tanaka N, Jonas JB, et al. Ultrawide-field OCT to investigate relationships between myopic macular retinoschisis and posterior staphyloma. *Ophthalmology*. 2018;125(10):1575–1586.
19. Panozzo G, Mercanti A. Optical coherence tomography findings in myopic traction maculopathy. *Arch Ophthalmol*. 2004;122(10):1455–1460.
20. Ohno-Matsui K, Shimada N, Yasuzumi K, et al. Long-term development of significant visual field defects in highly myopic eyes. *Am J Ophthalmol*. 2011;152(2):256–265.
21. Ohno-Matsui K, Kawasaki R, Jonas JB, et al. International photographic classification and grading system for myopic maculopathy. *Am J Ophthalmol*. 2015;159(5):877–883.e7.
22. Ishii K, Iwata H, Oshika T. Quantitative evaluation of changes in eyeball shape in emmetropization and myopic changes based on elliptic Fourier descriptors. *Invest Ophthalmol Vis Sci*. 2011;52(12):8585–8591.
23. Xie H, Chen Q, Yu J, et al. Morphologic features of myopic choroidal neovascularization in pathologic myopia on swept-source optical coherence tomography. *Front Med (Lausanne)*. 2020;7:615902.
24. Hsiang HW, Ohno-Matsui K, Shimada N, et al. Clinical characteristics of posterior staphyloma in eyes with pathologic myopia. *Am J Ophthalmol*. 2008;146(1):102–110.
25. Steidl SM, Pruett RC. Macular complications associated with posterior staphyloma. *Am J Ophthalmol*. 1997;123(2):181–187.

Investigative Ophthalmology & Visual Science